

## Compression of Carbon Nanotubes Filled with C<sub>60</sub>, CH<sub>4</sub>, or Ne: Predictions from Molecular Dynamics Simulations

Boris Ni,<sup>1</sup> Susan B. Sinnott,<sup>1,\*</sup> Paul T. Mikulski,<sup>2</sup> and Judith A. Harrison<sup>2</sup>

<sup>1</sup>*Department of Materials Science and Engineering, University of Florida, Gainesville, Florida 32611*

<sup>2</sup>*Department of Chemistry, U.S. Naval Academy, Annapolis, Maryland 21402*

(Received 11 September 2001; revised manuscript received 15 March 2002; published 6 May 2002)

The effect of filling nanotubes with C<sub>60</sub>, CH<sub>4</sub>, or Ne on the mechanical properties of the nanotubes is examined. The approach is classical molecular dynamics using the reactive empirical bond order (REBO) and the adaptive intermolecular REBO potentials. The simulations predict that the buckling force of filled nanotubes can be larger than that of empty nanotubes, and the magnitude of the increase depends on the density of the filling material. In addition, these simulations demonstrate that the buckling force of empty nanotubes depends on temperature. Filling the nanotube disrupts this temperature effect so that it is no longer present in some cases.

DOI: 10.1103/PhysRevLett.88.205505

PACS numbers: 62.25.+g, 31.15.Qg, 81.70.Bt

In the past few years there has been considerable interest in filling carbon nanotubes (CNTs) with various materials, such as noble gases [1–4], organic molecular gases such as CH<sub>4</sub> [5–8], and hydrogen [9–11]. In these studies, the ends of the CNTs are opened via chemical processes to facilitate filling [12]. Luzzi and co-workers have found that opening CNTs with acid creates defects (holes) in the CNT walls that allow C<sub>60</sub> molecules to enter their interior [13–15]. When the CNTs are annealed, the ends are closed, the defects are removed, and the resulting “nanopeapods” are found to contain strings of C<sub>60</sub> molecules [15].

In this paper, the effects of temperature and of filling single-walled CNTs with C<sub>60</sub>, CH<sub>4</sub>, or Ne on the compressibility of the CNTs are examined using classical molecular dynamics simulations. Previous computational papers have studied the compression and deformation of empty CNTs in free space [16–22] and pressed against surfaces [23–25]. At room temperature single-walled CNTs buckle to relieve the applied stress via a finning mechanism and have large Young’s moduli along the CNT axis. These properties have sparked interest in using CNTs as fibers in CNT-polymer matrix composites [26,27].

For the Ne-filled tubes, the forces in these simulations are calculated using Brenner’s reactive empirical bond-order (REBO) potential [28] for the short-range (covalent) interactions within the CNT walls and Lennard-Jones (LJ) potentials [29] for the Ne-carbon and the Ne-Ne interactions. The REBO potential realistically describes the properties of molecular and solid-state carbon materials, including bond energies, bond lengths, and lattice constants [28]. However, because the atoms are treated as hard spheres, forces from electronic effects, such as orbital resonance and symmetry, are neglected. The adaptive intermolecular REBO (AIREBO) potential, developed by Harrison and co-workers [20], is used for the CH<sub>4</sub>-filled and the C<sub>60</sub>-filled tubes. The AIREBO potential builds in accurate, long-range intermolecular interactions using LJ potentials to the REBO potential while maintaining its ability to model chemical reactions [28]. The AIREBO

LJ parameters have been shown to be able to reproduce condensed-phase properties, such as density, in a wide range of hydrocarbon liquids. These potentials have been used in related studies of the mechanical properties of [16–18,22,23,25], chemical functionalization of [31], and the diffusion of gases through [8,32] CNTs. Time steps in the range of 0.2–0.3 fs are used, depending on the system.

The CNTs considered are (10,10) single-walled tubes that are either 100 or 200 Å long and capped (with a C<sub>5v</sub> hemispherical cap [23]) at both ends. Every CNT is partitioned into three regions: the outer 92 atoms on each end are held rigid; moving toward the center of the CNT, the next 182 atoms (next to the rigid atoms) have independent Langevin heat baths [33] applied to them to maintain the temperature of the system; the remaining atoms are free to evolve in time with no additional constraints. Compression of the CNT is simulated by moving the rigid atoms at one end toward the other end with a constant velocity of 41 m/s. The instantaneous forces on the moving rigid-cap atoms are monitored. The compression rate is chosen so that there is sufficient time to dissipate excess energy to maintain a constant temperature, and fast enough to make the simulations computationally feasible. Temperatures between 140 and 1500 K are considered. In each case, five simulation trajectories are run and the resulting forces on the ends of the CNT due to the compression are smoothed, averaged, and plotted as a function of strain.

In the case of C<sub>60</sub>, densities of 0.752 g/cm<sup>3</sup> [8 (16) C<sub>60</sub> in the 100 Å (200 Å) CNTs], referred to as low density, 0.790 g/cm<sup>3</sup> (18 C<sub>60</sub> in the 200 Å CNTs), or medium density, and 0.940 g/cm<sup>3</sup> (10 C<sub>60</sub> in the 100 Å CNTs), or high density, are examined. In the case of Ne, densities of 0.431 g/cm<sup>3</sup> [330 (660) atoms in the 100 Å (200 Å) CNTs], referred to as low density, and 0.862 g/cm<sup>3</sup> [660 (1320) atoms in the 100 Å (200 Å) CNTs], or high density, are considered. In the case of CH<sub>4</sub>, one density of 0.292 g/cm<sup>3</sup> [140 (280) molecules in the 100 Å (200 Å) CNTs] is used.

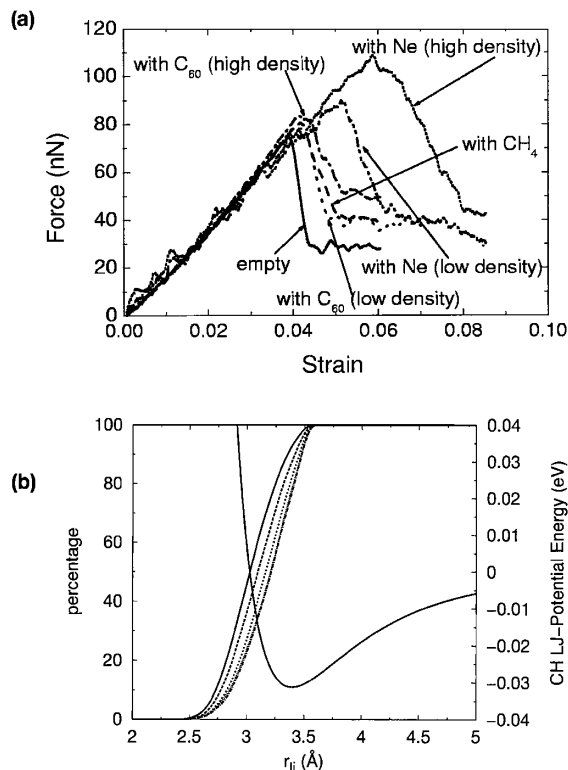


FIG. 1. (a) Force versus strain for the compression of empty and filled 100 Å CNTs at 300 K. (b) Percentage of C-H non-bonded interactions with a given interatomic separation calculated near the buckling point of the 100 Å CNT. From left to right in the figure the lines represent simulations with 140 (solid line), 120 (dashed line), 100 (dotted line), 80 (dash-dotted line), and 60 (which is indistinguishable from the 80 molecule line) CH<sub>4</sub> molecules. The AIREBO, C-H LJ function is included for comparison.

The force-strain curves from the compression of 100 Å CNTs that are empty and filled with C<sub>60</sub>, CH<sub>4</sub>, or Ne at various densities at 300 K are shown in Fig. 1a. In each case, the force increases as the CNT is compressed until it buckles. Further compression results in additional buckles that correspond to the smaller oscillations in the force-strain data at large values of strain. Because the forces from independent simulations are averaged at each value of strain, the standard deviation of the force at each point is also calculated. Regardless of the filling material, filled CNTs have significantly higher buckling forces compared to empty CNTs. With the exception of Ne, examination of the standard deviation of the forces at each strain demonstrates that there are no statistically significant differences between filling types at low densities. Filling with CH<sub>4</sub> or C<sub>60</sub> at low density increases the buckling force of the CNT approximately 3% to 13% (using the minimum and maximum standard deviations of the force). Filling with Ne at low density increases the buckling force of the CNT approximately 19% to 24%. An even larger increase in the buckling force (approximately 44% to 47%) is achieved by increasing the density of Ne to the high density.

These data suggest that it may also be possible to affect statistically significant changes in the buckling force by in-

creasing the number of C<sub>60</sub> molecules from 8 (low density) to 10 (high density). The average buckling force for the CNTs filled with C<sub>60</sub> at high density is larger than it is at low density. However, the variation in the forces among independent runs is large in the C<sub>60</sub> system at low density because the CNT buckles in different locations during independent simulations. Thus, it is not clear whether the difference observed in the average force for the two C<sub>60</sub> systems is statistically significant.

In an effort to elucidate the effect of filling density on the buckling force, multiple simulations of the CH<sub>4</sub>-filled, 100 Å CNT were run. The number of molecules in each simulation ranges from 2 to 140 molecules. The C-H and H-H nonbonded distances are analyzed in the buckling region for each density examined. These simulations show that the buckling force of the filled CNTs is approximately constant until a critical filling density is reached. When the CNT is filled with approximately 100 molecules, the buckling force begins to increase with increasing density. The origin of this behavior is apparent from an examination of Fig. 1b, where the percentage of the total C-H LJ interactions in the CH<sub>4</sub>-filled CNTs is plotted versus intermolecular separation. The AIREBO, LJ potential for C-H is also shown for comparison. It is clear that increasing the molecular density increases the number of molecules undergoing extremely repulsive interactions (the average C-H distance decreases). This increase is responsible for the increase in the buckling force once the critical density has been reached. Similarly, the fraction of LJ interactions along the repulsive wall of the H-H LJ potential increases as the density of CH<sub>4</sub> molecules increases.

The Young's modulus of the CNTs can be determined by dividing the values of the slopes of the force-strain curves shown in Fig. 1a by the cross-sectional area of the CNTs [16,17,34–37]. Several approaches for calculating the cross-sectional area of a CNT have been proposed in the literature [16,17,34–37], with the calculated value of Young's modulus depending strongly on the method chosen. Without calculating a modulus value, it is clear from examination of the curves in Fig. 1a that the slopes of the curves prior to buckling are approximately equal. (As it is clear from Fig. 1a that the Young's modulus is unaffected by filling we do not calculate the Young's modulus here.) Therefore, filling a CNT does not alter its Young's modulus but will affect quantities such as its flexural modulus [38].

The deformation behavior during compression when the 100 Å CNTs are filled with Ne, CH<sub>4</sub>, or C<sub>60</sub> at low densities is very similar to the deformation of an empty CNT [17]. Because of the flexibility of the CNT along its axis, one or more buckles develop in the tube when the buckling force is reached. At low densities, the gas atoms or molecules are able to easily rearrange themselves to avoid being forced into close proximity with each other or the CNT walls. The analysis of the effect of CH<sub>4</sub>-filling density discussed above demonstrates that the magnitude of

the buckling force is governed by the repulsive interactions among the molecules and between the molecules and the CNT.

Comparison of the buckling force of the high-density Ne-filled CNT with the high-density  $C_{60}$ -filled CNT reveals that these forces are quite different for the two species. The Ne atoms are small and can pack inside the CNTs in three dimensions. As a result, the average LJ distance between the atoms is small, with average intermolecular separations of 2.52–2.62 Å at low density and 2.33–2.38 Å at high density. Thus, a larger fraction of the Ne-Ne LJ interactions are farther up the repulsive wall of the potential at higher density, and the buckling force is larger at higher density. The motion of the  $C_{60}$  inside the tubes is essentially restricted to one dimension. While changing the number of molecules in the 100 Å CNT from 8 to 10 forces the buckyballs into closer proximity, it does not change the average LJ separation significantly. As a result, the majority of the LJ interactions occur at distances that are not as far up the repulsive wall as they are in the Ne-filled tube. Therefore, the buckling force changes only slightly for the two  $C_{60}$  densities examined here, and the overall buckling force is smaller for the  $C_{60}$ -filled tubes than for the Ne-filled tubes.

These data clearly show that the position and slope of the repulsive region of the intermolecular potential functions used dictate the magnitude of the buckling force observed in a given simulation. Because the magnitude of the buckling force depends on the choice of intermolecular potential, the results reported here are qualitative in nature. The repulsive wall of the Ne-Ne LJ potential used compares favorably to an exp-6 potential [39,40] that has been shown to correctly reproduce the experimental equation of state for high-pressure Ne [40] up to an interatomic separation of 2.47 Å. At distances smaller than 2.47 Å, the Ne-Ne LJ potential becomes slightly more repulsive than the exp-6 potential. With this in mind, if an exp-6 potential [39,40] were used to study the compression of Ne-filled CNTs instead of the LJ potential used here, the buckling force of the high-density Ne-filled CNT would differ from the number reported here. However, the same trends of buckling force with density would be observed.

In the case of the  $CH_4$ -filled and  $C_{60}$ -filled CNTs, a number of parameter sets for C-H, C-C, and H-H have been published in the literature for exp-6 and 9-6 potential energy functions [41]. Comparison of the AIREBO, LJ C-C, C-H, and H-H potentials to the exp-6 and 9-6 potentials of [42] reveals that the position of the repulsive wall in these potentials can be very close, as they are in the case of H-H, or differences can be somewhat larger, as they are in the case of C-H. In the case of the C-H potential, the repulsive wall of the LJ used here begins at larger internuclear separations than it does with the exp-6 potential. From this, one can conclude that simulations for  $CH_4$ -filled CNTs conducted with exp-6 potentials would show the same qualitative trends in buckling force. However, the increase in buckling force would be manifest at a

different (presumably larger) critical density. Conversely, if the position of the repulsive wall is at larger internuclear separations than the potentials used here, as it is for the C-C exp-6 and 9-6 potentials, the critical density for  $C_{60}$ -filled tubes is likely to shift to lower values.

More recently, the mechanics of  $C_{60}$  in CNTs has been investigated [43]. In that paper, the LJ potential for  $C_{60}$ - $C_{60}$  interactions was compared to a Morse-type potential derived from density functional theory, local density approximation (DFT-LDA) calculations. The LJ potentials were found to be too hard in the repulsive region of the potential. That is, the slope of the repulsive region of the DFT-LDA potential was less than the LJ potentials. Because the repulsive wall region was still present in the DFT-LDA potential, it is clear that the phenomenon reported here would still occur.

To assess how temperature affects the buckling force of the filled CNTs, the simulations discussed above are repeated over a range of temperatures between 100 and 1500 K. The buckling force of the empty tube decreases as the temperature increases (see Fig. 2a). The change in the buckling force becomes more dramatic with increasing

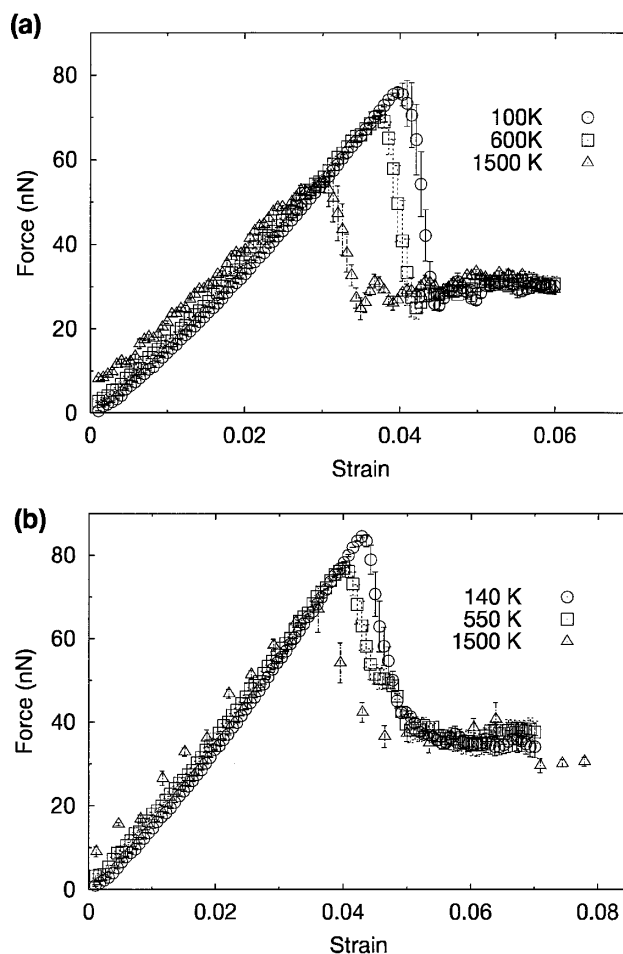


FIG. 2. Force versus strain curves at the indicated temperatures for the compression of (a) empty 100 Å CNTs and (b) 100 Å CNTs filled with  $C_{60}$  at low density. The error bars represent one standard deviation.

temperature. Because the CNTs collapse by developing buckles in the tube walls, it appears that the increased thermal motion of the tube walls as the temperature is increased aids the buckling.

Filling the CNTs appears to disrupt the temperature effect. For the CH<sub>4</sub>-filled CNTs, there are no statistically significant differences in buckling forces at 140, 300, 550, and 1500 K and in the case of the Ne-filled CNTs there are no differences in buckling forces at 140, 300, and 550 K. However, there are small, but significant, differences in the buckling force in the case of the CNTs filled with C<sub>60</sub> at low density, as shown in Fig. 2b. If the increased thermal motion of the CNT wall at higher temperatures aids the buckling process (Fig. 2a), filling the tube with many light atoms or molecules (Ne or CH<sub>4</sub>) that undergo multiple collisions with the CNT walls appears to disrupt the concerted motion needed to initiate buckling. Alternatively, it may also be the filling material and its intermolecular interactions that govern the buckling behavior, rather than the properties of the CNT alone. In contrast, fullerenes are more massive and there are fewer fullerene molecules, and fewer repulsive interactions, inside the CNTs. Thus, they undergo fewer collisions with the CNT walls and so do not disrupt the concerted buckling process as much as the other filling materials.

For reasons similar to those discussed above, filling the longer CNTs increases the amount of compression necessary to reach the buckling force for all filling species and filling does not affect the value of Young's modulus. The mechanisms that lead to the higher buckling force for the filled 200 Å CNTs are similar to the mechanisms in the filled 100 Å CNTs. The 200 Å CNTs considered bend rather than buckle [17]. However, at low densities the filling atoms (molecules) are still able to rearrange themselves to avoid the bending region. This gives confidence that the findings presented above are generally applicable to filled CNTs of even longer lengths than those considered in the simulations.

B. N. and S. B. S. acknowledge the support of the NASA Ames Research Center. P. T. M. and J. A. H. acknowledge the support of ONR and AFOSR under Contracts No. N00014-01-WR-20213 and No. NMIPR015-203507, respectively. The authors thank S. J. Stuart and K.-H. Lee for helpful discussions and technical assistance.

---

\*Author to whom correspondence should be addressed.

Email address: sinnott@mse.ufl.edu

- [1] M. K. Kostov *et al.*, Chem. Phys. Lett. **322**, 26 (2000).
- [2] M. W. Cole *et al.*, Phys. Rev. Lett. **84**, 3883 (2000).
- [3] W. Teizer *et al.*, Phys. Rev. Lett. **84**, 1844 (2000).
- [4] A. Kuznetsova *et al.*, Chem. Phys. Lett. **321**, 292 (2000).
- [5] S. Talapatra *et al.*, Phys. Rev. Lett. **85**, 138 (2000).
- [6] M. Muris *et al.*, Langmuir **16**, 7019 (2000).

- [7] M. Bienfait *et al.*, Surf. Sci. **460**, 243 (2000).
- [8] Z. Mao and S. B. Sinnott, J. Phys. Chem. B **104**, 4618 (2000).
- [9] M. Rzepka, P. Lamp, and M. A. de la Casa-Lillo, J. Phys. Chem. B **102**, 10 894 (1998).
- [10] M. S. Dresselhaus, K. A. Williams, and P. C. Eklund, MRS Bull. **24**, 45 (1999).
- [11] P. A. Gordon and R. B. Saeger, Ind. Eng. Chem. Res. **38**, 4647 (1999).
- [12] J. Liu *et al.*, Science **280**, 1253 (1998).
- [13] B. W. Smith, M. Monthieux, and D. E. Luzzi, Nature (London) **396**, 323 (1998).
- [14] B. Bouteaux *et al.*, Chem. Phys. Lett. **310**, 21 (1999).
- [15] B. W. Smith and D. E. Luzzi, Chem. Phys. Lett. **321**, 169 (2000).
- [16] C. F. Cornwell and L. T. Wille, Solid State Commun. **101**, 555 (1997).
- [17] B. I. Yakobson, C. J. Brabec, and J. Bernholc, Phys. Rev. Lett. **76**, 2511 (1996).
- [18] S. Iijima *et al.*, J. Chem. Phys. **104**, 2089 (1996).
- [19] D. Srivastava, M. Menon, and K. Cho, Phys. Rev. Lett. **83**, 2973 (1999).
- [20] M. B. Nardelli, B. I. Yakobson, and J. Bernholc, Phys. Rev. B **57**, R4277 (1998).
- [21] B. I. Yakobson, Appl. Phys. Lett. **72**, 918 (1998).
- [22] S. B. Sinnott *et al.*, Carbon **36**, 1 (1998).
- [23] J. A. Harrison *et al.*, J. Phys. Chem. B **101**, 9682 (1997).
- [24] N. Yao and V. Lordi, Phys. Rev. B **58**, 12 649 (1998).
- [25] A. Garg, J. Han, and S. B. Sinnott, Phys. Rev. Lett. **81**, 2260 (1998).
- [26] P. M. Ajayan *et al.*, Science **265**, 1212 (1994).
- [27] C. Bower *et al.*, Appl. Phys. Lett. **74**, 3317 (1999).
- [28] D. W. Brenner *et al.*, J. Phys. Condens. Matter **14**, 783 (2002).
- [29] M. P. Allen and D. J. Tildesley, *Computer Simulation of Liquids* (Oxford University Press, New York, 1987).
- [30] S. J. Stuart, A. B. Tutein, and J. A. Harrison, J. Chem. Phys. **112**, 6472 (2000).
- [31] B. Ni and S. B. Sinnott, Phys. Rev. B **61**, R16343 (2000).
- [32] Z. Mao and S. B. Sinnott, J. Phys. Chem. B **105**, 6916 (2001).
- [33] D. Frenkel and B. Smit, *Understanding Molecular Simulation: From Algorithms to Applications* (Academic Press, San Diego, 1996).
- [34] Z. Xin, Z. Jianjin, and O.-Y. Zhong-can, Phys. Rev. B **62**, 13 692 (2000).
- [35] V. N. Popov and V. E. V. Doren, Phys. Rev. B **61**, 3078 (2000).
- [36] E. Hernandez *et al.*, Phys. Rev. Lett. **80**, 4502 (1998).
- [37] J. P. Lu, Phys. Rev. Lett. **79**, 1297 (1997).
- [38] D. O. Brush and B. Almroth, *Buckling of Bars, Plates, and Shells* (McGraw-Hill, New York, 1975).
- [39] M. Ross *et al.*, J. Chem. Phys. **85**, 1028 (1986).
- [40] R. J. Hemley *et al.*, Phys. Rev. B **39**, 11 820 (1989).
- [41] G. Gilippini, C. M. Gramaccioli, and M. Simonetta, J. Chem. Phys. **73**, 1376 (1980).
- [42] Z. Gamba and H. Bonadeo, J. Chem. Phys. **76**, 6215 (1982).
- [43] D. Qian, W. K. Lin, and R. S. Ruoff, J. Phys. Chem. B **105**, 10 753 (2001).